Progress In Electromagnetics Research, Vol. 122, 437–452, 2012

ELECTROMAGNETIC OPTIMAL DESIGN FOR DUAL-BAND RADOME WALL WITH ALTERNATING LAYERS OF STAGGERED COMPOSITE AND KAGOME LATTICE STRUCTURE

Y. M. Pei[1,*], A. M. Zeng[2], L. C. Zhou[1], R. B. Zhang[1], and K. X. Xu[2]

[1]State Key Lab for Turbulence and Complex Systems, College of Engineering, Peking University, Beijing 100871, China

[2]School of Aerospace Engineering, Beijing Institute of Technology, Beijing 100081, China

Abstract—In this paper, electromagnetic optimal design is carried out for dual-band radome wall with alternating layers of staggered composite and Kagome lattice structure. The novel wall structure provides broadband transmission capability, along with excellent thermal-elastic properties and mechanical performances for high temperature applications. By optimizing the layer number (n) and the thickness of the whole wall (d), the power transmission efficiency of the novel structure in the frequency range of 1–100 GHz is calculated via boundary value method (BVM) based on electromagnetic theory. The calculation results suggest that if the wall thickness is dimensioned to be 6 mm and the wall structure is designed as 5 layers, the novel structure demonstrates excellent transmission performance. The optimal design results show that the power transmission efficiency is higher than 80% from 1 to 31 GHz in the centimeter wave range and from 59 to 100 GHz in the millimeter wave range, and the average transmission efficiency over the pass band reaches as high as 91%.

1. INTRODUCTION

A radome, an acronym coined from radar dome, is a cover or structure placed over an antenna that protects the antenna from its physical environment [1–3]. Ideally, the radome must allow transmission of electromagnetic waves and does not degrade the

Received 19 October 2011, Accepted 30 November 2011, Scheduled 6 December 2011

* Corresponding author: Yongmao Pei (peiym@pku.edu.cn).

electrical performances of the enclosed antenna in any way. It can be manufactured into a desired shape and is widely applied in marines, aircraft, missiles, and other vehicles carrying radar. Structural integrity of the radome competes with its electromagnetic transparency and the level of competition depends on the requirements related to a particular application environment. Thus, optimal design for the wall structure is needed [4, 5].

Usually, radome wall constructions include half wavelength wall, thin wall, sandwich wall and multilayer wall [6–8]. The half wavelength wall possesses performances meeting the normal radome applications, but it has relatively narrow bandwidth of about 5%. The thin wall radome requires a thickness less than 5% wavelength of the operating frequency in order to obtain satisfactory transmission capability. So it finds little aircraft applications above X-band, since the wall would be too thin to have enough mechanical strength [9, 10]. Multilayer or sandwich radome wall which offers a high strength-to-weight ratio satisfies the need for increased operating bandwidth [11]. Previously, Mackenzie and Stressing disclosed a radome wall construction, an A-sandwich construction, which included a sandwich of impact resistant thermoplastic closed cell foam core bounded by epoxy/quartz laminate facings [12]. The facings were dimensioned to be a half wavelength wall for a 94 GHz wave and thin wall for a 9.345 GHz wave. The radome construction was used for Boeing 727/737/747 aircraft radome and air transport aircraft while maintaining satisfactory transmission efficiency for both the X-band radar and W-band radar. Fig. 1(a) shows the prior art A-sandwich construction. Fig. 1(b) is a computational plot of the transmission efficiency of the A-sandwich construction as shown in Fig. 1(a). The transmission and reflection of electromagnetic waves through a plate are basically affected by the relationship between wavelength and thickness of the plate. Such relationship will vary periodically when the frequency increases, therefore, leading to periodic spikes in power transmission coefficient curve of the plate. It is noted that although the A-sandwich has relatively good transmission efficiency for both the X-band and W-band, the bandwidth in the frequency range is relatively narrow.

For high speed applications, the radome structure must provide appropriate weight, mechanical performances and thermal shock resistance. Multilayer or sandwich structures made of two different phases exhibit good fracture toughness, which can be 2–3 times larger than that of the homogeneous materials, while keeping higher bending strength [13]. However, thermal shock resistance of these sandwich structures might be not so good, since the different coefficient of thermal expansions (CTEs) between the two phases will lead to

thermal mismatch stress. Current researches find that staggered microstructure from bio-materials possesses better mechanical and thermal-elastic properties, since the thermal mismatch stress between staggered composite and the environment material or structure can be efficiently reduced [14, 15]. Additionally, Kagome lattice structure can provide the most optimum multifunctional performances, such as elastic properties, improved mechanical strength, and ease of fabrication at a specified structural weight [16].

Taking into account the advantages of the staggered composite and Kagome lattice structure mentioned above, we report a novel multilayer structure with alternating layers of staggered composite and Kagome lattice structure, aiming at better transmission performance with better thermal-elastic and mechanical properties. The odd layer made of staggered composite is dimensioned to be a half wavelength wall for a 90 GHz millimeter wave and thin wall for a 9 GHz centimeter

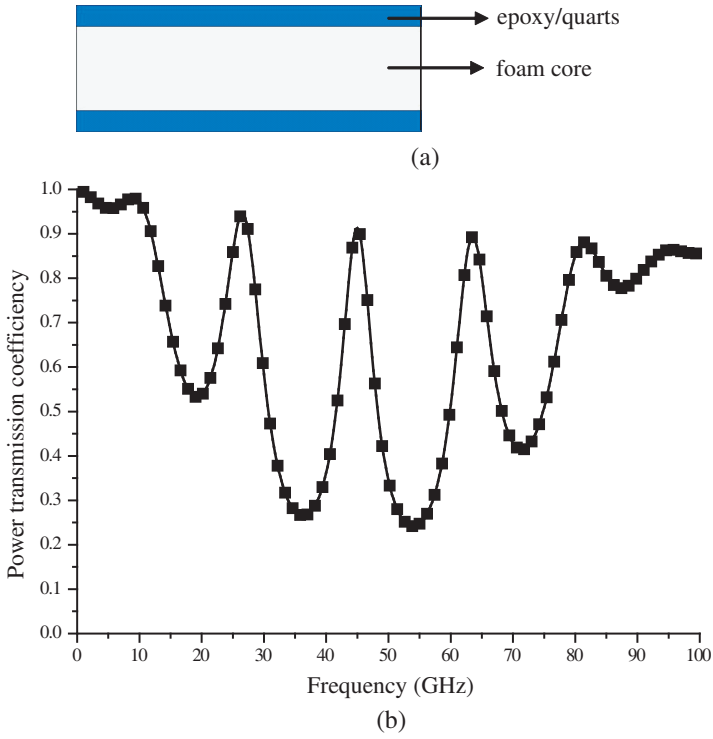

Figure 1. (a) Schematic section of a prior art A-sandwich radome wall construction. (b) Transmission efficiency verses frequency of the A-sandwich construction as shown in (a) over the range of 1–100 GHz.

wave. The even layer, which is electromagnetically similar to free space, is made of Kagome lattice structure with a higher strength-to-weight ratio. A homogenization method is adopted to evaluate the dielectric constant, for both the staggered composite and Kagome lattice structure. By optimizing the layer number (n) and the thickness of the whole wall (d), the power transmission efficiency of the multilayer structure with alternating layers in the frequency range of 1–100 GHz is calculated via boundary value method. Results show that the novel construction is feasible for dual-band radome used in both centimeter and millimeter wave ranges, and the transmission capability is efficiently elevated compared to traditional construction.

2. NOVEL CONSTRUCTION AND METHODS

2.1. Novel Multilayer Construction with Alternating Layers

In order to obtain broadband transmission capability, we present a new radome construction as shown in Fig. 2. The construction actually presents a multilayer structure compared to the three-layer structure in Fig. 1(a). The novel construction is symmetric and has odd layer

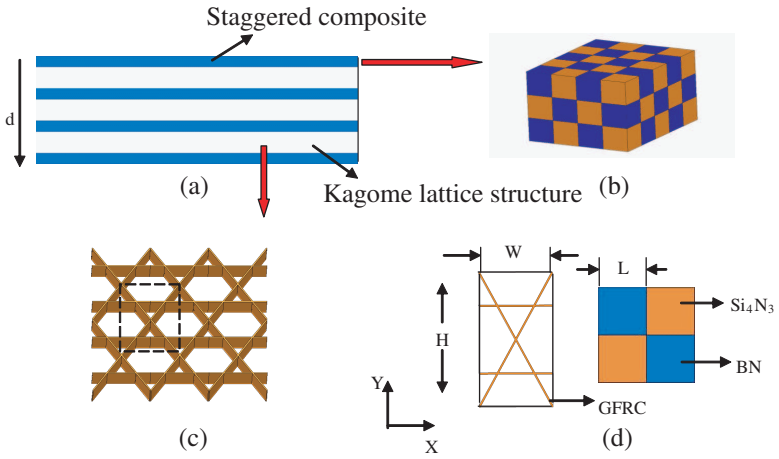

Figure 2. The novel Alternating Layers of Staggered Composite and Kagome Lattice Structure. (a) Mathematical model. (b) Schematic diagram of the checkerboard mixture, a three dimensional 0-0 type binary mixture. (c) Schematic diagram of the 2-D Kagome lattice grids. (d) Unit cell of Kagome structure and staggered composite in x-y plane.

number (n). Staggered composite, which has better thermo-elastic properties, is chosen to form the odd layer. The staggered composite consists of two different phases which have different dielectric constant and dielectric loss (loss tangent), as can be seen in Fig. 2(b). It represents a 0-0 type of connectivity, where both phases are distributed as checkerboard type of three-dimensional structure and both are non-connected. Typically, the even layer is made of foam material which is electromagnetically similar to free space. Kagome lattice structure, as shown in Fig. 2(c), is chosen to form the even layer, for the fact that it has relatively low density and better mechanical properties. The effective dielectric constant of the Kagome lattice structure can be controlled through varying the wall thickness of Kagome cell.

2.2. Homogenization Method for Estimating the Equivalent Dielectric Constant

To estimate the equivalent dielectric property of staggered composite, a versatile formula which contains many predictions of the effective dielectric constant is adopted [17]:

$$\frac{\varepsilon_{ff} - \varepsilon_1}{\varepsilon_{ff} + 2\varepsilon_1 + v(\varepsilon_{ff} - \varepsilon_1)} = f\frac{\varepsilon_2 - \varepsilon_1}{\varepsilon_2 + 2\varepsilon_1 + v(\varepsilon_{ff} - \varepsilon_1)} \tag{1}$$

where ε_1 is the dielectric constant of the environment, ε_2 is the dielectric constant of the inclusions, f is the volume fraction of the inclusion phase and ε_{ff} is the equivalent dielectric constant. Different values of the parameter v lead to various mixing rules: $v = 0$ gives the fundamental Maxwell Garnett rule [18], $v = 2$ gives the Bruggeman formula [19], and $v = 3$ returns the so-called coherent potential approximation. Even though all these rules are limited to the conditions that the inclusions are spherical and small compared with the wavelength of the operating electromagnetic field, results given in Refs. [20, 21] indicate that the homogenization models can be accurate for periods as large as 1/2 to 1 free space wavelength, and possibly even larger for lossy structures. Often, these mixing formulas are applied to a wider class of mixtures with reasonable success, especially when the dielectric contrast $k = \varepsilon_2/\varepsilon_1$ is small, such as 3 [22, 23].

For the checkerboard type of composite analyzed in this paper, the homogenization formula achieves reliable dielectric constant if the parameter v is 1.5 [24]. Considering extreme aerodynamic stresses and loading requirement, the staggered composite must have higher density. Here we can choose Si_4 N_3 and BN to form the staggered composite which has been manufactured and verified to possess better mechanical performances and thermal-elastic behaviors [25–27]. Plastic forming methods, including extrusion and roll compaction,

respectively, followed by hot-pressed sintering can be used to prepare ceramic staggered composites [28]. By controlling the porosity, the ceramic can be manufactured into a material with desired electromagnetic and mechanical properties. As porous Si_4N_3 with a dielectric constant of 2.8 satisfies the mechanical requirements, here we choose the dielectric constant and dielectric loss of Si_4N_3 as 2.8 and 0.002 respectively. And we choose 4.1 and 0.006 as the dielectric constant and dielectric loss of BN. In this case, the effective dielectric constant and dielectric loss of the staggered composite obtained from Eq. (1) are approximately 3.4 and 0.0038 respectively.

Honeycomb composite of hexagonal lattice geometry similar with Kagome is analyzed in Ref. [29] by using Hashin-Shtrikman (HS) upper bound to estimate the effective dielectric property, where the agreement between the HS upper bound and the finite element method (FEM) results is excellent. The maximum relative error compared to the HS upper bound is less than 1% over the entire interval. At the same time, effective conductivity of Kagome lattice structure is indeed predicted using HS upper bound, which also agrees well with the topology optimization results [16]. It is pointed out that results obtained for the effective electrical conductivity translate immediately into equivalent results for the effective dielectric constant, thermal conductivity, and magnetic permeability for reasons of mathematical analogy [16]. Consequently, we choose

$$\varepsilon_{ff} = \varepsilon_s \frac{(2-f)\varepsilon_0 + f\varepsilon_s}{f\varepsilon_0 - (2-f)\varepsilon_s} \tag{2}$$

as a proper best-fit, where ε_s and ε_0 are the complex dielectric constant of bulk material and free vacuum.

The Kagome lattice structure is made of glass fiber reinforced composite (GFRC) which has the dielectric constant and dielectric loss of 2.7 and 0.04. The Interlocked Composite Grid and Extrusion molding process are mainly manufacturing methods to make Kagome lattice structure [30, 31]. In this paper, the structural parameters H, W and L shown in Fig. 2(d) are designed as 2.7 mm, 1.56 mm and 0.3 mm respectively, so the volume fraction of GFRC of the Kagome lattice structure is chosen as 0.04. Therefore, the effective dielectric constant and dielectric loss of the Kagome lattice structure can be calculated as 1.05 and 0.001 by HS upper bound.

The thickness of the staggered composite layer which has higher density and dielectric constant is normally 0.762 mm or greater in order to provide sufficient structural properties [1]. A staggered composite layer of 0.9 mm in thickness meets the requirements of a half wavelength wall for a 90 GHz wave and a thin wall for a 9 GHz wave. Therefore, each odd layer of the proposed construction in this

paper is dimensioned to be 0.9 mm in thickness, in order to form a dielectric matching layer with sufficient mechanical properties. For calculation of power transmission efficiency of the multilayer structure with alternating layers of staggered composite and Kagome lattice structure, the effects of the dielectric constant and dielectric loss of each layer, the layer number, the thickness of each layer should be taken into consideration. Based on the fact that the material of each layer and the thickness of the staggered composite layer have been decided, and the even layer of Kagome lattice structure is assumed to be equal in thickness, we only need to consider the whole thickness of the wall and layer number of the structure.

2.3. The Boundary Value Method for Calculating the Transmission Efficiency

Before calculations of power transmission efficiency, some hypotheses are made as follows:

(1) Plane wave solutions are used in mathematical descriptions of wave propagation in order to synthesize more complicated wavefronts.

(2) The theory of plane wave propagation through a plane dielectric sheet is used for radome design because a curved radome can be approximated as locally planar. This paper describes propagation vertical into flat sheets only.

(3) Permittivity and dielectric loss of each material keep invariable at the whole calculation bandwidth.

The analysis of microwave transmission for a flat multilayer lamination can be achieved via a boundary value solution of the N-layer dielectric wall, the solution takes the form [32, 33]:

$$\begin{bmatrix} E_0^+ \\ E_0^- \end{bmatrix} = \left[\prod_{i=1}^{N} \frac{1}{T_i} \begin{pmatrix} e^{j\gamma_i t_i} & R_i e^{-j\gamma_i t_i} \\ R_i e^{+j\gamma_i t_i} & e^{-j\gamma_i t_i} \end{pmatrix}\right] \frac{1}{T_{N+1}} \begin{bmatrix} 1 & R_{N+1} \\ R_{N+1} & 1 \end{bmatrix} \begin{bmatrix} E_{N+1}^+ \\ 0 \end{bmatrix} \quad (3)$$

where E_0^+, E_0^- and E_{N+1}^+ represent the amplitudes of electric fields of the incident wave, reflected wave and transmitted wave respectively, t_i is the thickness of the ith layer, R_i and T_i are Fresnel reflection and transmission coefficients at the interface between the $(i-1)$th and ith layers. γ_i is the propagation constant normal to the boundary within the ith layer, as given by

$$\gamma_i = k_0 \sqrt{\varepsilon_{ri}} \cos\theta_i \quad (4)$$

in which ε_{ri} is the relative permittivity of the ith layer (a complex quantity), k_0 is the wave number in free space, and θ_i is the ray angle within the ith layer measured with respect to the surface normal.

The angle in each layer can be found from the well-known Snell's law:

$$\theta_i = \sin^{-1}\left(\frac{\sqrt{\varepsilon_{r(i-1)}}}{\sqrt{\varepsilon_{ri}}}\sin\theta_{i-1}\right) \tag{5}$$

By carrying out the matrix multiplication in Eq. (2) and gathering terms together, the equation can then be written as:

$$\begin{bmatrix} E_0^+ \\ E_0^- \end{bmatrix} = \begin{bmatrix} A_{11} & A_{12} \\ A_{21} & A_{22} \end{bmatrix} \begin{bmatrix} E_{N+1}^+ \\ 0 \end{bmatrix} \tag{6}$$

The transmission voltage coefficient is given by

$$T_w = \frac{1}{A_{11}} \tag{7}$$

Both the reflection coefficient and the transmission coefficient are complex and can be expressed in terms of its magnitude and the insertion phase delayer (IPD) angle.

The power transmission efficiency can be rewritten as

$$|T_W|^2 = \left|\frac{1}{A_{11}}\right|^2 \tag{8}$$

3. RESULTS AND DISCUSSION

An acceptable transmission efficiency usually requires a 70% minimum transmission efficiency, preferably at least 80%, and most preferably at least 85% transmission efficiency average over the frequency range. In this study, we consider the acceptable minimum transmission efficiency greater than 80%. As discussed in Section 2.2, the effective dielectric constant and dielectric loss of each material have been estimated: $\varepsilon_1 = 3.4$, $\delta_1 = 0.0038$, $\varepsilon_2 = 1.05$ and $\delta_2 = 0.001$. The thickness of each odd layer has also been decided as $d_1 = 0.9\,\text{mm}$. The effects of the whole thickness and the layer number of the structure are to be discussed below.

Firstly, we are going to optimize the layer number of the structure. The initial condition for the wall thickness is $d = 6\,\text{mm}$.

The effect of the layer number (n) on the transmission efficiency of the novel multilayer structure in the frequency range of 1–100 GHz is shown in Fig. 3. It is well known that multilayer radomes which include low-density core materials and higher-density skin materials are popular, because multilayer radomes have wider bandwidth and a higher strength-to-weight ratio than monolithic radomes. However, as the layer number increases, the whole thickness of staggered composite layers with high dielectric constant also increases, which will decrease

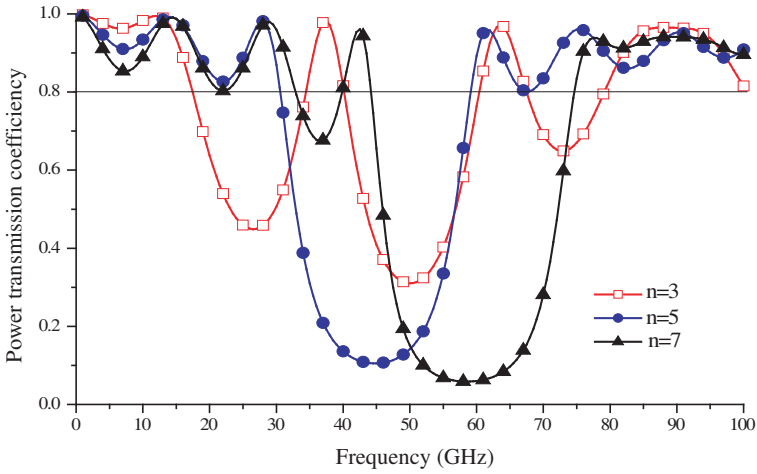

Figure 3. Power transmission efficiency of the novel alternate structure as functions of the layer number in the frequency range of 1–100 GHz.

the power transmission efficiency. So, optimizing the number of layers which possess broadband properties with sufficient structural strength is necessary. According to Fig. 3, if the structure is designed as 3 layers, the structure has higher power transmission efficiency at passband, but the bandwidth is narrow; if the structure is designed as 7 layers, it has broader bandwidth at low frequency band, but bandwidth at high frequency band is not wide enough; only if the layer number is designed as 5, it can obtain broadband capability at both low and high frequency bands. It can be seen that the power transmission efficiency is more than 80% at frequency range of 1–31 GHz and 59–100 GHz. Thus, we choose $n = 5$ as the optimal layer number of the structure.

Secondly, the effect of the whole thickness of the radome wall is taken into consideration. Taking into account that a certain thickness is needed for mechanical requirements, we only discuss the case of wall thickness greater than 6 mm. The initial condition is taken as $n = 5$.

Figure 4 shows the effect of the wall thickness (d) on the transmission efficiency of the multilayer structure with alternating layers in the frequency range of 1–100 GHz. According to Fig. 4, as d increases from 6 to 10 mm, the bandwidth of passband decreases gradually. When the thickness increases from 6 mm, the bandwidth at high frequency band becomes narrower significantly, while the bandwidth at low frequency band is slightly extended as the wall thickness decreases. It is obviously seen that the proposed structure

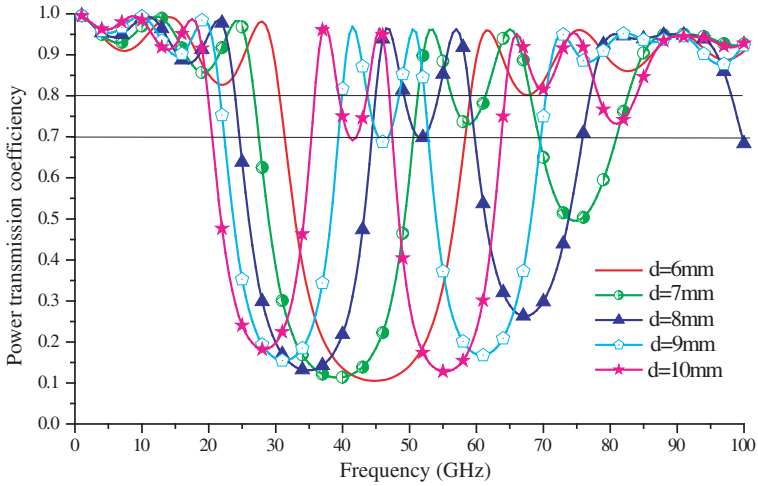

Figure 4. Power transmission efficiency of the novel alternate structure as functions of the whole wall thickness in the frequency range of 1–100 GHz.

possesses the best broadband capability when the wall is 6 mm thick. The transmission efficiency is all greater than 80% except the frequency range from 31 to 59 GHz. Thus, the most optimal wall thickness of the novel multilayer structure radome is chosen as 6 mm according to the discussion above. If the transmission efficiency is required to be above 70%, we can see in Fig. 4 that the radome wall which thickness is about $7 \sim 8$ mm can be used in three-band applications.

From the above calculations we could conclude that, if the wall structure is 6 mm thick with 5 alternating layers, the structure obtains the best broadband transmission efficiency. The power transmission efficiency is higher than 80% at frequency range of 1–31 GHz and 59–100 GHz, and the transmission efficiency average over the frequency range reach as high as 91%, which meets the requirements of broadband radome.

Figure 5 shows the transmission efficiency of the optimum design structure over the range from 1 to 100 GHz by finite element simulation software HFSS and the boundary value method. The computational speed of BVM is much faster than that of HFSS. While BVM takes only 3 seconds, HFSS may expend 30 minutes or so because the micro-structure is modeled directly in FEM simulation. The micro-structural parameters of the subunits shown in Fig. 2(d) are $H = 2.7$ mm, $W = 1.56$ mm, and $L = 0.3$ mm respectively in HFSS. It can be obviously seen that the results calculated by the two different methods

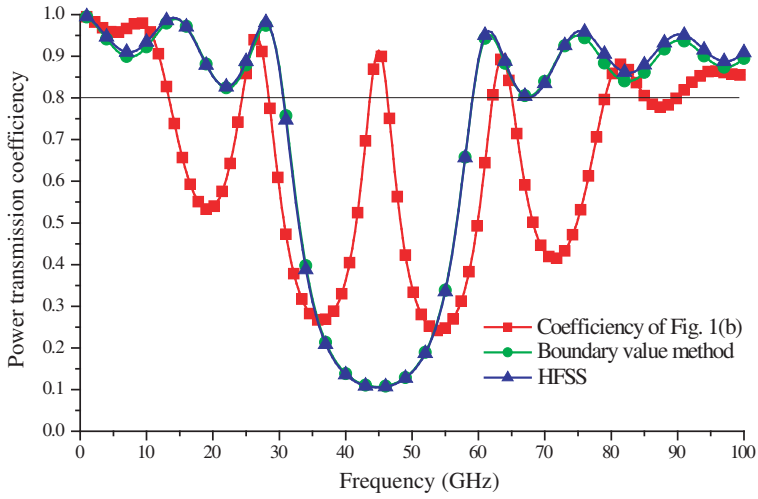

Figure 5. Power transmission efficiency of the optimal structure calculated by simulation software HFSS and BVM in the frequency range of 1–100 GHz.

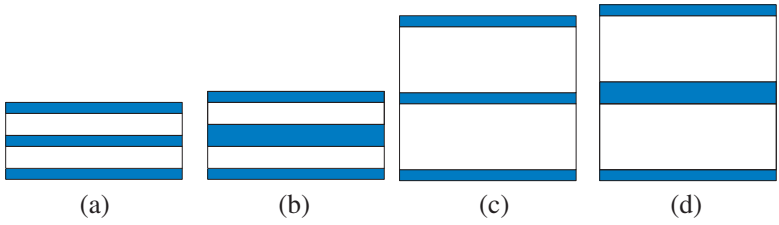

Figure 6. (a) Novel alternate structure. (b) Double-intermediate-layer structure. (c) A-quarter-wavelength structure. (d) Mixed structure.

agree fairly well. Comparing to Fig. 1(b), it is seen that the bandwidth both in the centimeter and millimeter wave ranges of the proposed structure in this paper is much broader than that of the construction from Ref. [9], namely construction of Fig. 1(a).

In a typical symmetric structure of five layers, namely C-sandwich radome structure, the intermediate layer is typically made to be about twice the susceptance of the inner and outer skin layers for electrical reasons [34]. The susceptance of each layer is a function of the dielectric constant of the material, its thickness, and the frequency of interest. If the same material is used for all three layers, the intermediate layer is typically twice as thick as the inner or outer skin layers. Meanwhile,

the even layer of the C-sandwich structure, electromagnetically similar to free space, has a thickness of approximately a quarter wavelength for optimum cancellation of reflections caused by high dielectric constant layer, namely approximately 8 mm. Fig. 6 presents four kinds of C-sandwich radome structures with different dimensions: the novel structure (Model a) shown in Fig. 6(a) is the structure proposed in this paper; double-intermediate-layer structure (Model b) shown in Fig. 6(b) has an intermediate layer twice as thick as that of the novel structure; a-quarter-wavelength structure (Model c) shown in Fig. 6(c) has core layer (even layer) of a quarter wavelength thick compared to the novel structure; mixed structure (Model d) shown in Fig. 6(d) has both double-thick intermediate layer and core layer of a quarter wavelength thick. Fig. 7 shows the transmission efficiency over the range from 1 to 100 GHz for four different structures mentioned above. It is seen that the novel structure has the best broadband transmission efficiency among the four structures. We can see that structures with uniform thickness of intermediate layer and outmost skin layer have better broadband capability, compared to structures with intermediate layer as twice thick as outmost skin layer. Although a-quarter-wavelength structure and mixed structure possess greater power transmission efficiency in their passband, the bandwidth is relatively narrow. Among the four constructions, we can see that the novel structure of dual-band radome obtains the best transmission capability.

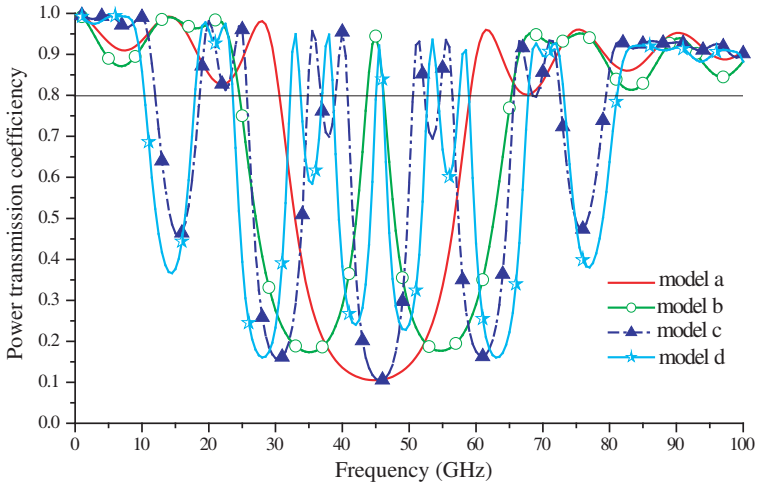

Figure 7. Transmission efficiency verses frequency of the four structures as shown in Fig. 6 over the range of 1–100 GHz.

4. CONCLUSION

In this study, a novel multilayer radome wall structure with alternating layers of staggered composite and Kagome lattice structure is proposed. The multilayer structure is designed to satisfy broadband requirement for centimeter and millimeter waves dual-band applications, along with better thermal-elastic behaviors and mechanical performances. The homogenization theory is adopted to estimate the effective dielectric constant of the staggered composite and Kagome lattice structure. And the power transmission efficiency of the construction is calculated via boundary value method. Calculations indicate that if the radome wall is dimensioned as 6 mm in thickness with 5 alternating layers, the construction achieves the best broadband transmission performance. The optimal result shows that the power transmission efficiency is higher than 80% at frequency range of 1–31 GHz and 59–100 GHz, and the transmission efficiency average over the frequency range reaches as high as 91%. Compared to traditional C-sandwich radome structures, the novel construction possesses better broadband capability. Our calculation results suggest that the novel structure with alternating layers of staggered composite and Kagome lattice structure is feasible for dual-band radome applications.

It should be emphasized that all results are for normal incidence only and are theoretical in our work. We will do more work on the radome analysis techniques to predict a radome-enclosed antenna's performance, such as the geometric optics (GO) and physical optics (PO) methods, in which the non-normal incidence and polarization effects should be considered [35–37]. Experimental measurements to confirm accuracy of homogeneous approximation of synthesized radome material are another interest of our further research [38, 39].

ACKNOWLEDGMENT

This work is supported by National Natural Science Foundation of China (Grant No. 10802008, 11072003 and 11090331), National Basic Research Program of China (973 Program, 2010CB832701 and 2011CB610303), and Foundation of the Author of National Excellent Doctoral Dissertation of China (No. 201029).

REFERENCES

1. Kozakoff, D. J., *Analysis of Radome Enclosed Antennas*, Artech House, Norwood, MA, 1997.

2. Persson, K., M. Gustafsson, and G. Kristensson, "Reconstruction and visualization of equivalent currents on a radome using an integral representation formulation," *Progress In Electromagnetics Research B*, Vol. 20, 65–90, 2008.
3. Sukharevsky, O. I. and V. A. Vasilets, "Scattering of reflector antenna with conic dielectric radome," *Progress In Electromagnetics Research B*, Vol. 4, 159–169, 2008.
4. Mackenzie, S. B., "Radome wall design having broadband and mm-wave characteristics," US Pat, 5408244, Apr. 18, 1995.
5. Chen, F., Q. Shen, and L. Zhang, "Electromagnetic optimal design and preparation of broadband ceramic radome material with graded porous structure," *Progress In Electromagnetics Research*, Vol. 105, 445–461, 2010.
6. Sunil, S., K. S. Venu, S. M. Vaitheeswaran, and U. Raveendranath, "A modified expression for determining the wall thickness of monolithic half-wave radomes," *Microw. Opt. Techn. Lett.*, Vol. 30, No. 5, 350–352, 2001.
7. Kedar, A. and U. K. Revankar, "Parametric study of flat sandwich multilayer radome," *Progress In Electromagnetics Research*, Vol. 66, 253–265, 2006.
8. Kedar, A., K. S. Beenamole, and U. K. Revankar, "Performance appraisal of active phased array antenna in presence of a multilayer flat sandwich radome," *Progress In Electromagnetics Research*, Vol. 66, 157–171, 2006.
9. Rudge, A. W., G. A. E. Crone, and J. Summers, "Radome design and performance: A review," *Proceedings of 2nd military microwaves Conference*, London, Oct. 1981.
10. Tice, T. E., "Techniques for airborne radome design," USAF Report AFATL-TR-66-391, 1966.
11. Crone, G., A. Rudge, and G. Taylor, "Design and performance of airborne radomes: A review," *IEE Proceedings F on Communications, Radar and Signal Processing*, Vol. 128, No. 7, 451–464, 1981.
12. Mackenzie, S. B. and D. W. Stressing, "W-band and X-band radome wall," US Pat, 6028565, Feb. 22, 2000.
13. Wang, C. A., Y. Huang, Q. Zan, H. Guo, and S. Cai, "Control of composition and structure in laminated silicon nitride/boron nitride composites," *Journal of the American Ceramic Society*, Vol. 85, No. 10, 2457–2461, 2002.
14. Ji, B. and H. Gao, "Mechanical properties of nanostructure of biological materials," *Journal of the Mechanics and Physics of*

Solids, Vol. 52, No. 9, 1963–1990, 2004.

15. Yang, F., D. N. Fang, and B. Liu, "Thermal-elastic behaviors of staggered composites," *International Journal of Applied Mechanics*, Vol. 1, No. 4, 569–580, 2009.
16. Hyun, S. and S. Torquato, "Optimal and manufacturable two-dimensional, Kagome-like cellular solids," *Journal of Materials Research*, Vol. 17, No. 1, 137–144,2002.
17. A. Sihvola, *Electromagnetic Mixing Formulas and Applications*, IEE Electromagnetic Waves Series, Vol. 47, UK, 1999.
18. Garnett, J. C. M., "Colours in metal glasses and in metallic films," *Transactions of the Royal Society*, Vol. CCIII, 385–420, London, 1904.
19. Tuncer, E., Y. V. Serdyuk, and S. M. Gubalski, "Dielectric mixtures: Electrical properties and modeling," *IEEE Transactions on Dielectrics and Electrical Insulation*, Vol. 9, No. 5, 809–828, 1935.
20. Holloway, C. L. and E. F. Kuester, "A low-frequency model for wedge or pyramid absorber arrays-II: Computed and measured results," *IEEE Transactions on Electromagnetic Compatibility*, Vol. 36, No. 4, 307–313, 1994.
21. Holloway, C. L., P. McKenna, and R. DeLyser, "A numerical investigation on the accuracy of the use of homogenization for analyzing periodic absorbing arrays," *Proc. Int. Symp. Electromag. Theory*, 296–298, URSI, St. Petersburg, Russia, 1995.
22. Kanaun, S. K. and D. Jeulin, "The influence of spatial distributions of inhomogeneities on effective dielectric properties of composite materials," *Progress In Electromagnetics Research*, Vol. 2, 51–84, 1999.
23. Sun, W., K. Liu, and C. A. Balanis, "Analysis of singly and doubly periodic absorbers by frequency-domain finite-difference method," *IEEE Transactions on Antennas and Propagation*, Vol. 44, No. 6,798–805,1996.
24. Jylha, L. and A. Sihvola, "Approximations and full numerical simulations for the conductivity of three dimensional checkerboard geometries," *IEEE Transactions on Dielectrics and Electrical Insulation*, Vol. 13, No. 4, 760–764, 2006.
25. Shen, Z. J., Z. Zhao, H. Peng, et al., "Formation of tough interlocking microstructures in silicon nitrideceramics by dynamic ripening," *Nature*, Vol. 417, 266–269, 2002.
26. Peterson, I. M. and T. Y. Tien, "Effect of the grain boundary thermal expansion coefficient on the fracture toughness in silicon

nitride," *J. Am. Ceram. Soc.*, Vol. 78, No. 9, 2345–2352, 1995.

27. Riley, F. L., "Silicon nitride and related materials," *J. Am. Ceram. Soc.*, Vol. 83, No. 2, 245–265, 2000.
28. Wang, H., Y. Huang, Q. F. Zhang, and H. Guo, "Biomimetic structure design-a possible approach to change the brittleness of ceramics in nature," *Materials Science and Engineering C*, Vol. 11, 9–12, 2000.
29. Johansson, M., C. L. Holloway, and E. F. Kuester, "Effective electromagnetic properties of honeycomb composites, and hollow-pyramidal and alternating-wedge absorbers," *IEEE Transactions on Antennas and Propagation*, Vol. 53, No.2, 728–736, 2005.
30. Han, D. and S. W. Tsai, "Interlocked composite grids design and manufacturing," *Journal of Composite Materials*, Vol. 37, No. 4, 287–316, 2003.
31. Kim, T. D., "Fabrication and testing of thin composite isogrid stiffened panel," *Compos. Struct.*, Vol. 49, No. 1, 21–25, 2000.
32. Collin, R. E. and H. Chang, "Field theory of guided waves," *Physics Today*, McGraw-Hill, 1961.
33. Orfanidis, S. J., "Electromagnetic waves and antennas," Rutgers University, NJ, 2009.
34. Ziolkowski, F., "Lightweight c-sandwich radome fabrication," US Patent, 7463212, Dec. 9, 2008.
35. Meng, H. F. and W. B. Dou, "A hybrid method for the analysis of radome-enclosed horn antenna," *Progress In Electromagnetics Research*, Vol. 90, 213–233, 2009.
36. Lee, H. S., "Prediction of radome bore-sight errors using a projected image of source distributions," *Progress In Electromagnetics Research*, Vol. 92, 181–194, 2009.
37. Meng, H. F. and W. B. Dou, "Fast analysis of electrically large radome in millimeter wave band with fast multipole acceleration," *Progress In Electromagnetics Research*, Vol. 120, 371–385, 2011.
38. Eibert, T. F., Ismatullah, E. Kaliyaperumal, and C. H. Schmidt, "Inverse equivalent surface current method with hierarchical higher order basis functions, full probe correction and multi-level fast multipole acceleration," *Progress In Electromagnetics Research*, Vol. 106, 377–394, 2010.
39. Quijano, J. L. A. and G. Vecchi, "Field and source equivalence in source reconstruction on 3D surfaces," *Progress In Electromagnetics Research*, Vol. 103, 67–100, 2010.